



A direct methanol fuel cell system to power a humanoid robot

Han-Ik Joh^{a,b}, Tae Jung Ha^a, Sang Youp Hwang^a, Jong-Ho Kim^a, Seung-Hoon Chae^a,
Jae Hyung Cho^a, Joghee Prabhuram^a, Soo-Kil Kim^a, Tae-Hoon Lim^a,
Baek-Kyu Cho^c, Jun-Ho Oh^c, Sang Heup Moon^{b,*}, Heung Yong Ha^{a,**}

^a Center for Fuel Cell Research, Korea Institute of Science and Technology (KIST), P.O. Box 131, Cheongyang, Seoul 130-650, Republic of Korea

^b School of Chemical & Biological Engineering and Institute of Chemical Processes, Seoul National University, San 56-1, Shillim-dong, Kwanak-ku, Seoul 151-744, Republic of Korea

^c HUBO Laboratory, Humanoid Robot Research Center, Department of Mechanical Engineering,

Korea Advanced Institute of Science and Technology, 373-1 Guseong-dong, Yuseong-gu, Daejeon 305-701, Republic of Korea

ARTICLE INFO

Article history:

Received 27 May 2009

Received in revised form 7 July 2009

Accepted 8 July 2009

Available online 18 July 2009

Keywords:

Direct methanol fuel cell

Load sharing ratio

Efficiency

Fuel cell/battery hybrid system

Robot

ABSTRACT

In this study, a direct methanol fuel cell (DMFC) system, which is the first of its kind, has been developed to power a humanoid robot. The DMFC system consists of a stack, a balance of plant (BOP), a power management unit (PMU), and a back-up battery. The stack has 42 unit cells and is able to produce about 400 W at 19.3 V. The robot is 125 cm tall, weighs 56 kg, and consumes 210 W during normal operation. The robot is integrated with the DMFC system that powers the robot in a stable manner for more than 2 h. The power consumption by the robot during various motions is studied, and load sharing between the fuel cell and the back-up battery is also observed. The loss of methanol feed due to crossover and evaporation amounts to 32.0% and the efficiency of the DMFC system in terms of net electric power is 22.0%.

© 2009 Elsevier B.V. All rights reserved.

1. Introduction

Direct methanol fuel cells (DMFCs) are considered to be a potential power source for mobile and portable applications, such as cellular phones, notebook PCs, and portable electronic devices [1–4]. Efforts to commercialize DMFCs as a portable power system are summarized in Table 1 [1,3–12]. However, some of the unresolved issues, such as poor reliability, durability, high costs, and low power density remain to be obstacles in the commercialization process. Hence, many efforts have been made to improve the performance of the membrane-electrode assembly (MEA) and the stack of the DMFC: modifying the structure of Nafion membrane [13,14], developing more active catalysts [15,16], optimizing the operational conditions [4,17], and improving the stack design [3,18–21] to increase the power and energy density of DMFCs. In this study, the DMFC was employed as a power source for humanoid robots by improving the stack design and optimizing the operation parameters of the DMFC system.

The development and design of robots have recently gained momentum, because robots are capable of performing various kinds of work normally carried out by human beings. For example, a robot developed by Korea Advanced Institute of Science and Technology (KAIST), which is popularly known as HUBO, can perform various kinds of activities. An important issue in the development of humanoid robots is the efficient provision of electric power. HUBO is currently powered by a set of secondary batteries, and the robot can be operated for only about 60 min. In order to increase the operating duration of the robot, the power provided by the secondary batteries has to be supplemented by other power sources that can deliver power for a longer period.

This study focused on the practical aspects of the DMFC/battery hybrid system to power the humanoid robot. Load sharing between the fuel cell and the battery was also studied during various dynamic motions of the robot. The efficiency of the DMFC was calculated on the basis of changes in the current and the voltage.

2. Experimental

The robot center at KAIST collaborated with the DMFC team at KIST to power a humanoid robot using the DMFC/battery hybrid system. The humanoid robot, HUBO, is 125 cm tall, weighs 55 kg, and has 41 degrees of freedom (DOF). The robot was equipped earlier with a Li-ion battery as a source of electric power, and was sub-

* Corresponding author. Tel.: +82 2 880 7409; fax: +82 2 875 6697.

** Corresponding author. Tel.: +82 2 958 5275; fax: +82 2 958 5199.

E-mail addresses: shmoon@surf.snu.ac.kr (S.H. Moon), hyha@kist.re.kr, hyha88@hotmail.com (H.Y. Ha).

Table 1
Prototype DMFC systems developed by several companies and research institutes.

Company or Institute	Power [W]	System volume [ml]	Fuel volume [ml]	Application
Chen C.Y. [1]	20	N/A	N/A	DVD & Note PC
KIST [3]	50	N/A	N/A	LCD TV
KIER [4]	40	N/A	N/A	Portable Power Supply
Toshiba [5]	12	825	N/A	Laptop PC
NEC [6]	14	N/A	300	Laptop PC
Fujitsu [7]	15	N/A	300	Laptop PC
LG Chem. [9]	25	1000	200	Laptop PC
Matsushita Battery Industrial (MBI) [10]	13	400	200	Laptop PC
Antig Tech. [11]	45	N/A	N/A	Laptop PC
Samsung Advanced Institute of Technology (SAIT) [8]	N/A	N/A	100	Laptop PC
SAIT [12]	2	150	N/A	Portable Power Supply

N/A.: not available.

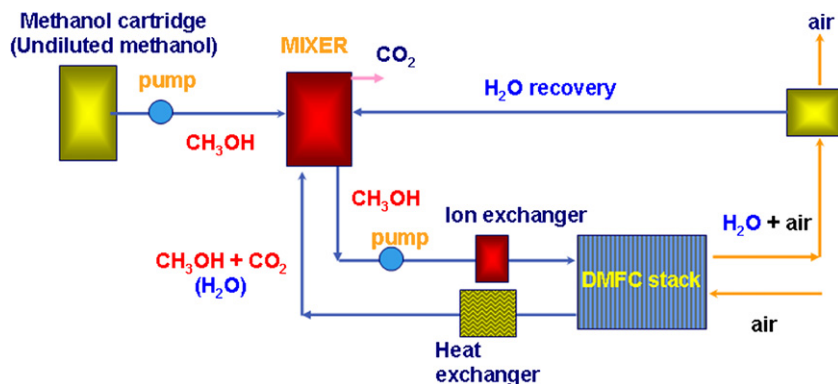


Fig. 1. A flow diagram of the DMFC system.

jected to modification by the team at KAIST to accommodate the DMFC system.

The DMFC/battery hybrid system consisted of a stack, a balance of plant (BOP), a power management unit (PMU), and a back-up battery. A Nafion 115 membrane was used as the polymer electrolyte for the fabrication of membrane-electrode assemblies (MEAs). The catalyst loadings in the anode and the cathode were 6.0 mg cm^{-2} of PtRu black and 4.0 mg cm^{-2} of Pt black (Johnson–Matthey), respectively. Machined graphite bipolar plates with a serpentine flow field

were used. The performance of the stack was tested under various operating conditions to determine the optimum conditions for the DMFC system [22].

The BOP comprised three liquid pumps, an air blower, a methanol mixer, a methanol reservoir, gas–liquid separators, valves, and heat exchangers. The three liquid pumps were used for supplying pure methanol to the methanol mixer, methanol feed to the stack, and for recirculating collected water from the cathode side heat exchanger to the methanol mixer. In order to control the

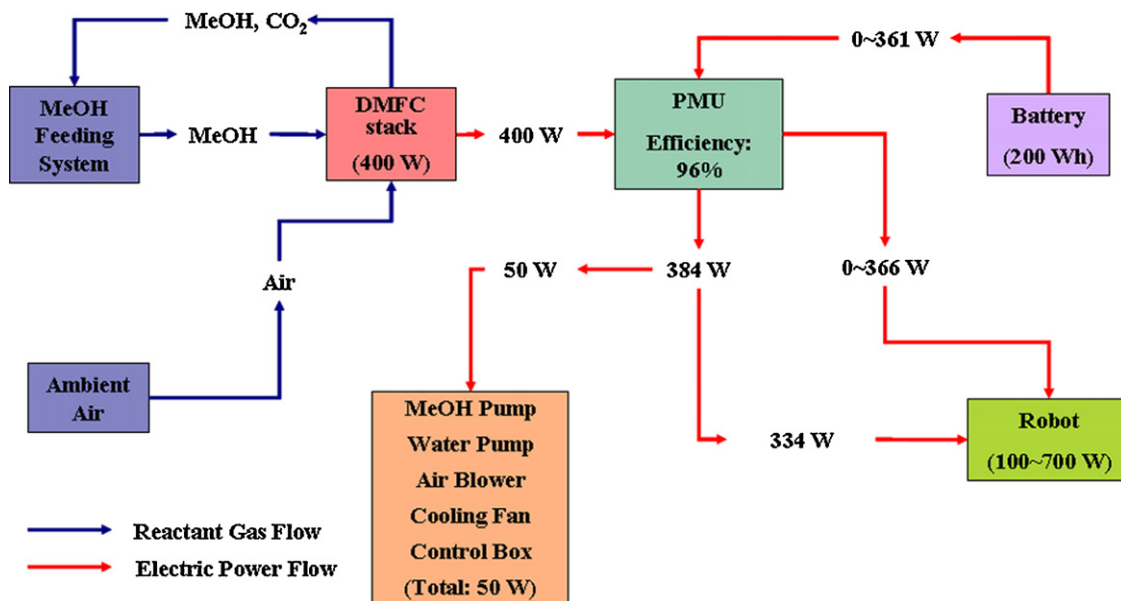


Fig. 2. A flow diagram of the DMFC/battery hybrid system.

concentration of methanol feed, we developed a methanol control system that did not use methanol sensors. Therefore, methanol sensors were not included in this DMFC system [23]. The sensor-less methanol concentration controller (SLCC) was designed to maintain a constant concentration of recirculating methanol feed by adding the exact amount of methanol into the feed stream that was consumed during the operation of the stack. In order to achieve this, a methanol consumption map was developed, which could be determined by measuring the methanol consumption rates at all the operating conditions used in the DMFC system. A calculated amount of pure methanol from the reservoir was added to the recirculating feed stream by means of a micro-pump. The dosing rate of pure methanol varied with the size, properties, and temperature of the stack, and the amount of current produced by the stack. The details of the SLCC have been described elsewhere [23].

The PMU was equipped with a SLCC and a DC/DC converter. The PMU also acted as a central processing unit and controlled the operations of all the components in the DMFC system, as well as distributing electric power produced from the stack and the battery to the BOP and the robot. In order to measure the efficiency of the PMU, the output voltage from PMU was investigated when the power with constant voltage at 16 V (or 19 V, or 22 V) was supplied into the PMU using a power supply equipment.

A flow diagram of the DMFC system is shown in Fig. 1. A diluted methanol solution was fed into the anode and ambient air was supplied into the cathode of the DMFC stack. The methanol solution coming out of the stack went through a heat exchanger and lowered its temperature. The solution was then collected in the methanol mixer, where the concentration of solution was brought up to a given value by adding pure methanol from the methanol reservoir. The concentration of methanol solution in the mixer was controlled by the SLCC. Ambient air was fed into the cathode side of the stack using a blower, and the humidified hot air coming out of the stack went through a heat exchanger to precipitate water. Here, the collected water was sent to the methanol mixer to compensate for the loss of water that occurred at the anode.

A flow diagram for the generation of electric power in the DMFC/battery hybrid system is shown in Fig. 2. The DMFC stack was connected in parallel with a back-up battery, which could provide power if the total power required from the loads exceeded the capacity of the stack. The PMU managed the distribution of the electric loads between the DMFC stack and the battery.

3. Results and discussion

In order to determine the size of the DMFC power generator required for fabrication purposes, the power consumption required by the robot was tested while it was performing various kinds of activities. As shown in Fig. 3, the robot utilized 112, 420, and 720 W (this is not shown in Fig. 3) while standing still, walking, and performing multiple actions, respectively. In a normal operational mode like walking, the robot can consume 400 W, so the stack was designed with the capacity to generate about 400 W, which was adequate to cover the electric load required for the robot and the BOP, which consumed about 50 W as shown in Table 2, of the DMFC

Table 2
Specification of BOP components.

Components	Voltage [V]	Current [A]	Power [W]
Pump 1	24	0.325	7.8
Pump 2	24	0.096	2.3
Pump 3	24	0.096	2.3
3-Way valve	24	0.063	1.5
Fan	12	5	6
Blower	15	2	30
BOP total power	–	–	49.9

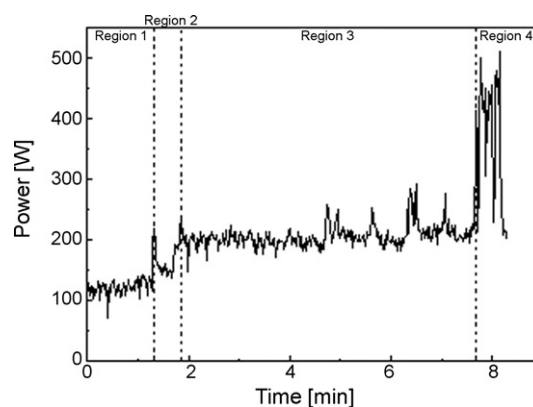


Fig. 3. Power consumption of the robot at various stages of motion: (1) and (2) warming-up and position adjustment, (3) stand-still or hand shaking, and (4) walking.

system. The maximum power derived, i.e., about 720 W, was backed up by a battery connected in parallel with the stack.

Several variables were taken into account in designing the dimensions of the DMFC stack, including the size of the MEAs and the number of unit cells accommodated in the stack. As the stack capacity can be obtained by multiplying the size of the MEAs and the number of the unit cells, they are in inverse proportion under a fixed electric power output. First, the voltage of the electricity produced from the stack under normal operating conditions was taken into consideration. In order to increase the efficiency of the DC/DC converter, which was usually in the range of 80–90%, the stack design was modified to produce higher voltages of about 18–20 V under normal operating conditions. Therefore, we have decided to use MEAs with an active area of 138 cm² and to pile up 42 unit cells to build a stack, which could generate a total of 19.3 V (0.46 V per unit cell) and about 400 W of power.

The stack was tested to find its optimal operating conditions, under which it could produce the desired amount of electric power and be operated stably with low degradation or without any malfunction. The concentration of methanol feed can affect the temperature, performance, and durability of the stack. Therefore, the temperature variation in the stack was first observed by circulating the methanol feed at a room temperature of 25 °C under open circuit conditions. Three different concentrations of methanol, i.e., 0.5, 0.8 and 1.0 M were fed to the anode. It was found that the 1.0 M feed raised the temperature of the stack to 80 °C, even under open circuit conditions. The temperature of the stack remained at 30 °C with the 0.8 M methanol feed and at 25 °C with the 0.5 M methanol feed. Therefore, it was decided to rule out using the 1.0 M feed, because the temperature of the stack could have risen higher than 80 °C during the course of the electrochemical reactions that generated heat and electric power in the stack [22].

In order to determine the optimal concentration of methanol, the performance of the stack was studied by using 0.5 and 0.8 M of methanol. Fig. 4 compares the performance of the stack using different concentrations of methanol. In these experiments, the flow rates of the reactants, methanol and air, were fixed based on the stoichiometries of 3.6/3.6 at a current density of 150 mA cm⁻². Under the given operating conditions, 0.8 M of methanol produced about 400 W of power, while 0.5 M of methanol could produce around 200 W of power. Therefore, we decided to use 0.8 M of methanol as fuel in the stack of the DMFC system.

Another big issue in DMFC systems is the maintenance of methanol feed concentration at a given value. The easiest method might be the use of a methanol sensor, but the state of the art methanol sensors are expensive and difficult to be accommodated into DMFC systems. Therefore, as mentioned in the experimental

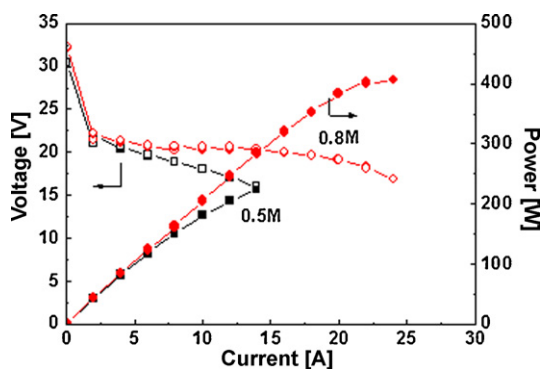


Fig. 4. Performance of the DMFC stack with different methanol feed concentrations.

section, a SLCC was used as shown in Fig. 5. In the initial stage of this experiment, the methanol concentration was permitted to drop to 0.3 M by allowing electrochemical reactions in the stack that could draw a current of around 20 A. Under these conditions, the SLCC was manually turned on to increase the feed concentration of methanol to reach the set value of 0.8 M. At first, the concentration exceeded the set point, but it soon dropped and the feed concentration reached the value of 0.8 M in 20 min. This ensured that the SLCC operated in an efficient manner and maintained the methanol feed concentration at the set point with a deviation of around 10%.

The temperature of a DMFC stack usually increases due to the heat released by the exothermic cathodic reaction and oxidation of crossed methanol at the cathode. Therefore, in this system a heat exchanger was used to quench the heated methanol solution coming out of the stack. As shown in Fig. 6, the temperatures

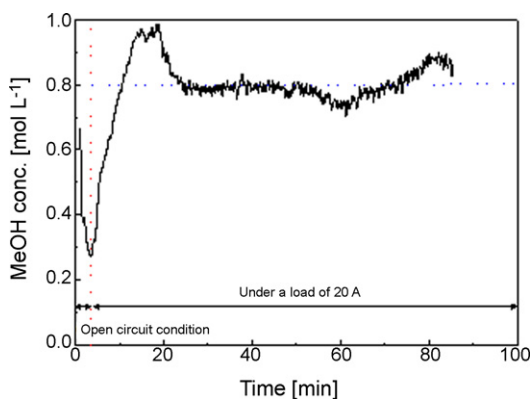


Fig. 5. Changes in the methanol feed concentration while it is controlled by the SLCC.

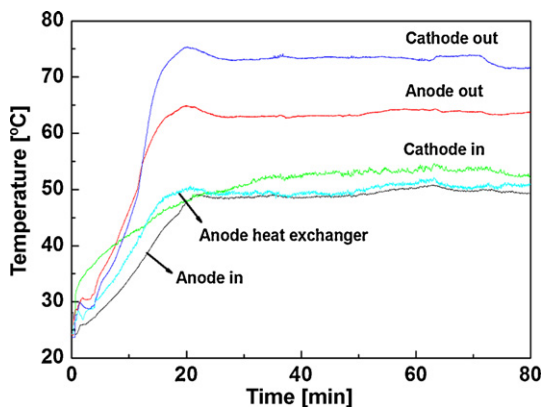


Fig. 6. Changes in the temperatures of the reactants that enter and exit the stack.

of the methanol solution and the air that entered and exited the stack were initially maintained at 25 °C. Since the methanol solution was being circulated through the stack, the temperature of the methanol solution from the stack ('anode out' in the figure) gradually increased similar to temperature of the methanol feed ('anode in'). The 'anode out' temperature rose above 50 °C in 12 min; then, the fan attached to the heat exchanger automatically switched on to keep the temperature of the methanol feed at 50 °C. Subsequently, in this experimental condition the temperature of the methanol feed declined to around 50 °C and the temperature of the methanol solution coming out of the stack was maintained at around 65 °C. The temperature of air at the cathode outlet was found to be 75 °C, which was higher than that of the methanol solution. The exothermic reaction at the cathode is responsible for the increase in temperature of the stack, even though the anodic reaction is endothermic.

In this DMFC system, the voltage of the DC electricity generated by the stack varied from 16 to 34 V, depending on the amount of current produced. In order to utilize the electricity, the voltage should be regulated to a constant reading of 28 V through a DC/DC converter. The PMU used in this study was a kind of micro-processor that functioned to regulate the DC voltage and control the operation of the BOP system, such as the valves, liquid pumps, air blowers, fans, and electric switches to route the electric power to various loads. Fig. 7 shows the efficiency of the power management unit that could transform the varying voltages (16–22 V) to a higher output of 28 V as the total electric power varied from 50 to 250 W. The efficiency of the converter is found to be around 95% for all the input voltages tested. If the input voltages are much lower than the target voltage, the efficiency can be reduced to below 90%. Therefore, in order to obtain higher efficiency, the voltage of electricity from the stack should be maintained as close to the target voltage as possible, by controlling the operating conditions or by increasing the number of cells in the stack.

After testing all the components in the DMFC system, the stack was integrated with the BOP, a PMU, and a battery to build a stand-alone DMFC/battery hybrid system on a breadboard. In this experiment, a 200 Wh Li-ion battery was employed for back-up power. The performance of the DMFC power generator was tested to determine whether it could be operated automatically and in a stable manner, without any malfunction, under various electric loads. To study the load sharing behavior between the stack and the battery, a set of experiments was designed and conducted using an artificial load that could simulate the robot's power consumption. As shown in Fig. 8(a), the electric load was increased stepwise from 5 to 15 A, while monitoring the power drawn from the stack and the battery. In this experiment, the electric power was consumed by the artificial load and the BOP. The load imposed by the BOP is not shown in this graph, but the artificial load (denoted as 'robot') plus

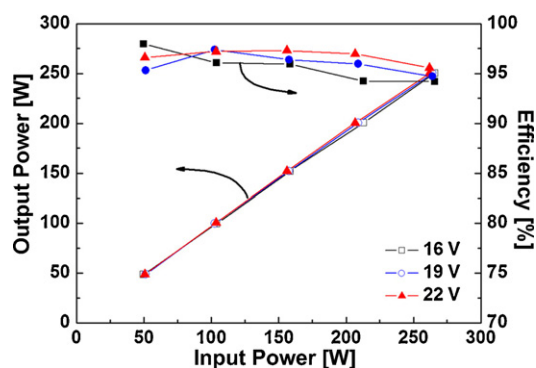


Fig. 7. Efficiency of the power management unit (PMU) at various input power and voltage.

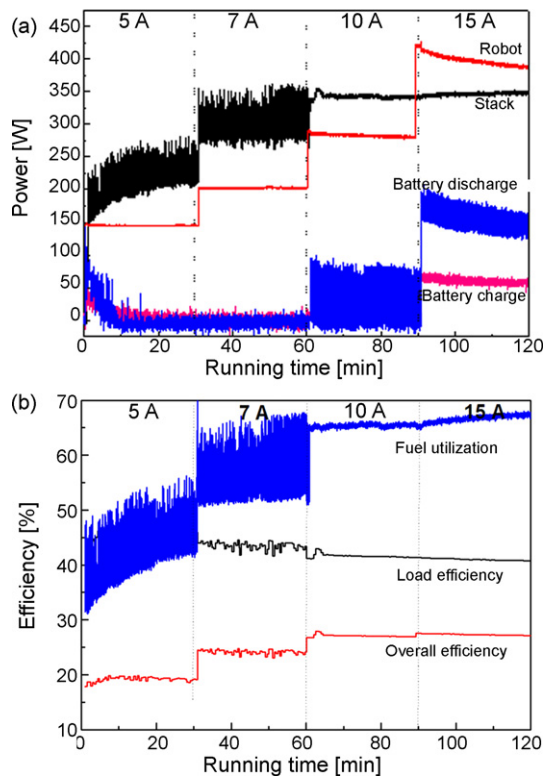


Fig. 8. Performance of the stand-alone DMFC/battery hybrid system at various electric loads: (a) load sharing between the stack and the battery and (b) efficiency of the hybrid system.

the BOP load is equivalent to the sum of the power drawn from the stack and the battery. At lower loads, i.e., below 10 A, all the loads could be rendered solely by the stack. At a higher load of 15 A, the stack was not able to deliver its full power, so part of it was supplied by the battery.

Fig. 8(b) shows the fuel utilization, load efficiency, and overall efficiency while power was drawn from the stack and the battery, as presented in Fig. 8(a). The fuel utilization was calculated based on the amount of methanol consumed and the corresponding power produced by the stack. The fuel utilization, η_{fuel} , was calculated as shown below:

$$\eta_{\text{fuel}} = \frac{W_C}{W_{\text{total}}} \times 100 \quad (1)$$

where W_C and W_{total} are the amount of methanol used to generate the given amount of power and the total amount of methanol consumed in the stack, respectively. The fuel utilization increased with increasing load, and reached around 68% at a load of 15 A. The load efficiency (η_{load}) was calculated on the basis of the voltages as follows:

$$\eta_{\text{load}} = \frac{V_C}{V_{Th}} \times 100 \quad (2)$$

where V_C and V_{Th} are the voltage of the cell and the theoretical voltage, respectively. The overall efficiency of the stack, η_{overall} , can be obtained as shown below:

$$\eta_{\text{overall}} = \eta_{\text{fuel}} \times \eta_{\text{load}} \quad (3)$$

As shown in Fig. 8(b), as the electric load increased the fuel utilization also increased, and, therefore, the overall efficiency improved. An overall efficiency of as high as 27.3% was attained when 15 A was drawn from the stack. As the electric load increased, the utilization of fuel increased, the loss of methanol was minimized, and, thus, the overall efficiency improved. In the stand-alone

DMFC/battery hybrid system, the DC/DC converter efficiency was found to be around 96.0% and the BOP and the PMU consumed a total of 50 W, as mentioned above. The BOP efficiency (η_{BOP}) was calculated and found to be 84.0%. This coincides with the fact that 16.0% of the power generated by the fuel cell stack was consumed to convert the DC voltage and to operate the BOP and the PMU.

After testing the stand-alone DMFC system and confirming its stable operation, the DMFC system was integrated with the robot. The empty space in the robot body was enlarged by restructuring the robot to accommodate the DMFC system. However, the space acquired by this modification was not sufficient, so a backpack had to be attached to the robot, as shown in Fig. 9. The modification of the robot was difficult, because the weight balance of the robot had to be maintained for stable operation. With trial-and-error the DMFC system, which has the weight of about 12 kg and the volume



Fig. 9. A picture of HUBO equipped with a DMFC power source.

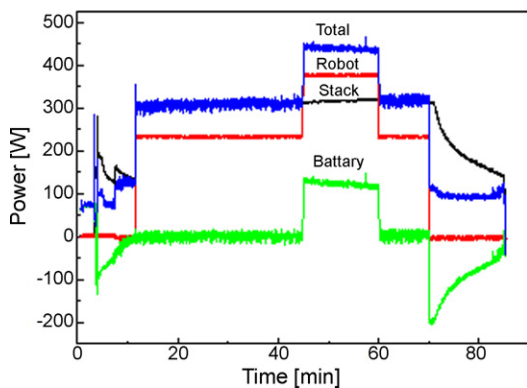


Fig. 10. Operation of the DMFC-powered robot, showing the load sharing between the DMFC stack and the battery.

of about 20 L, was successfully integrated and the robot could be operated in a stable manner. The robot could walk and perform various kinds of activities, as programmed, with power supplied by the DMFC system. The electric power consumption of the robot was monitored to determine how power was distributed while the robot performed different type of activities. Fig. 10 shows the power consumption in terms of electric current by the robot, and load sharing between the DMFC stack and the battery. In this figure, the difference between the total power and the power consumption by the robot is the power consumed by the BOP, including the PMU. At 10 min of operation, the power consumption by the robot was lower than the power produced by the DMFC stack. Under those conditions, the stack could render all the loads required by the BOP and the robot. Therefore, the total power consumption was equal to the power generated by the stack. After 45 min, when the robot was very active, it required more power than was supplied by the stack, which necessitated a portion of the power being supplied by the battery. At 70 min of operating time, when the robot was in an idle state, the power requirement dropped. At this stage, the surplus electricity produced from the DMFC was used to recharge the battery.

Another important factor is the performance of the power system, evaluated by calculating the total efficiency of the system. This can be defined as the ratio of the electrical energy produced to the chemical energy consumed. The total efficiency of the system, η_{system} , is as follows:

$$\eta_{\text{system}} = \eta_{\text{overall}} \times \eta_{\text{BOP}} \times \eta_{\text{DC/DC}} \quad (4)$$

Fig. 11 shows the breakdown of the chemical energy of methanol fuel that was consumed by the DMFC system to generate electricity. During the DMFC operation, 40.7% of the methanol was lost due to heat and electrochemical resistance in the course of fuel cell reac-

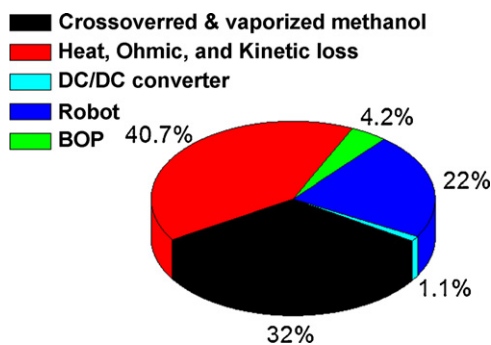


Fig. 11. A breakdown of the energy consumption in the DMFC system.

tions, 32.0% by methanol crossover and evaporation, and 5.3% was consumed by the BOP, including the DC/DC converter. Ultimately, the net electrical power (the total system efficiency) was found to be approximately 22.0%. Therefore, to increase the energy efficiency of the system, the methanol crossover should be minimized.

4. Conclusions

A DMFC system, the first of its kind, was developed to power a humanoid robot called HUBO (125 cm and 56 kg). The DMFC stack, comprised of 42 cells, showed very high and stable performance (150 mA cm^{-2} at 0.46 V , 70 mW cm^{-2} , 405 W). The volume of the DMFC system, however, was too big to insert into the open space of the robot's body, so the robot was equipped with a backpack to accommodate it. Therefore, to prevent DMFC-powered robots from becoming too large, either the volume of the DMFC system should be reduced, or the power density of the system should be enhanced. Another big issue with the DMFC system is the low energy efficiency due to methanol loss incurred by crossover and evaporation. In this DMFC system, the loss of methanol by crossover and evaporation amounted to 32.0% of the total methanol energy consumed, and the efficiency for the generation of net electric power was only 22.0%.

The DMFC-powered robot operated in a stable manner and demonstrated various kinds of activities. In fact, for the first time, the DMFC system has been successfully exploited to power humanoid robots. The DMFC system must evolve in such a way that the size is decreased and the energy efficiency is enhanced.

Acknowledgments

This work was financially supported by the Korean Ministry of Knowledge Economy through the Institute of Industrial Technology Evaluation and Planning (ITEP) under the research program: Industrial Technology Development Program. One of the authors, Dr. Joghee Prabhuram, thanks the Korean Federation of Science and Technology Societies (KOFST) and Korea Science and Engineering Federation (KOSEF) for support and assistance through the Brain Pool Program.

References

- [1] C.Y. Chen, D.H. Liu, C.L. Huang, C.L. Chang, J. Power Sources 167 (2007) 442–449.
- [2] C.Y. Chen, C.S. Tsao, Int. J. Hydrogen Energy 31 (2006) 391–398.
- [3] D. Kim, J. Lee, T.-H. Lim, I.-H. Oh, H.Y. Ha, J. Power Sources 155 (2006) 203–212.
- [4] B.-D. Lee, D.-H. Jung, Y.-H. Ko, J. Power Sources 131 (2004) 207–212.
- [5] Fuel Cells Bull. 5 (2003) 1.
- [6] Fuel Cells Bull. 8 (2003) 1.
- [7] Fuel Cells Bull. 3 (2004) 2.
- [8] Fuel Cells Bull. 6 (2004) 6.
- [9] Fuel Cells Bull. 11 (2005) 5.
- [10] Fuel Cells Bull. 3 (2006) 4.
- [11] Fuel Cells Bull. 5 (2006) 2–3.
- [12] Fuel Cells Bull. 2 (2007) 3.
- [13] M. Prasanna, E.A. Cho, H.-J. Kim, T.-H. Lim, I.-H. Oh, S.-A. Hong, J. Power Sources 160 (2006) 90–96.
- [14] P.L. Antonucci, A.S. Arico, P. Creti, E. Ramunni, V. Antonucci, Solid State Ionics 125 (1999) 431–437.
- [15] H.S. Liu, C.J. Song, L. Zhang, J.J. Zhang, H.J. Wang, D.P. Wilkinson, J. Power Sources 155 (2006) 95–110.
- [16] M. Gotz, H. Wendt, Electrochim. Acta 43 (1998) 3637–3644.
- [17] C.Y. Chen, P. Yang, Y.S. Lee, K.F. Lin, J. Power Sources 141 (2005) 24–29.
- [18] C.Y. Chen, J.Y. Shiu, Y.S. Lee, J. Power Sources 159 (2006) 1042–1047.
- [19] R. Jiang, C. Rong, D. Chu, J. Power Sources 126 (2004) 119–124.
- [20] H. Dohle, H. Schmitz, T. Bewer, J. Mergel, D. Stolten, J. Power Sources 106 (2002) 313–322.
- [21] D. Buttin, M. Dupont, M. Straumann, R. Gille, J.-C. Dubois, R. Ornelas, G.P. Fleba, E. Ramunni, V. Antonucci, A.S. Arico, P. Creti, E. Modica, M. Pham-Thi, J.-P. Ganne, J. Appl. Electrochem. 31 (2001) 275–279.
- [22] H.-I. Joh, S.Y. Hwang, J.H. Cho, T.J. Ha, S.-K. Kim, S.H. Moon, H.Y. Ha, Int. J. Hydrogen Energy 33 (2008) 7153–7162.
- [23] T.J. Ha, J.-H. Kim, H.-I. Joh, S.-K. Kim, G.-Y. Moon, T.-H. Lim, C. Han, H.Y. Ha, Int. J. Hydrogen Energy 33 (2008) 7163–7171.